Journal of Thermal Analysis and Calorimetry, Vol. 75 (2004) 233–248

CRYSTALLIZATION AND MELTING OF ISOTACTIC POLYPROPYLENE IN RESPONSE TO TEMPERATURE MODULATION

A. Genovese and R. A. Shanks[*]

Department of Applied Chemistry, RMIT University, GPO Box 2476V, Melbourne, Victoria 3001, Australia

(Received July 27, 2003; in revised form September 30, 2003)

Abstract

Isotactic polypropylene (iPP) was crystallized using temperature modulation in a differential scanning calorimeter (DSC) to thicken the crystals formed on cooling from the melt. A cool–heat modulation method was adopted for the preparation of the samples under a series of conditions. The effect of modulation parameters, such as temperature amplitude and period was monitored with the heating rate that followed. Thickening of the lamellae as a result of the crystallization treatment enabled by the cool–heat method lead to an increase in the peak melting temperature and the final traces of melting. For instance, iPP melting peak shifted by up to 3.5°C with temperature amplitude of 1.0°C while the crystallinity was increased from 0.45 (linearly cooled) to 0.53. Multiple melting endotherms were also observed in some cases, but this was sensitive to the temperature changes experienced on cooling. Even with a slower underlying cooling rate and small temperature amplitudes, some recrystallization and reorganization occurred during the subsequent heating scan. The crystallinity was increased significantly and this was attributed to the crystal perfection that occurred at the crystal growth surface. In addition, temperature modulated differential scanning calorimetry (TMDSC) has been used to study the melting of iPP for various crystallization treatments. The reversing and non-reversing contribution under the experimental time scale was modified by the relative crystal stability formed during crystallization. Much of the melting of iPP was found to be irreversible.

Keywords: crystallization, DSC, isotactic polypropylene, melting, TMDSC

Introduction

The crystallization and melting of polyolefin's has been a subject of much interest, particularly in the case of isotactic polypropylene (iPP). Multiple melting endotherms are commonly observed in differential scanning calorimetry (DSC) experiments. The origin of the multiple melting peaks in iPP has been attributed to factors such as crystallization temperature [1–4], heating rate, orientation [3], the presence of different crystal modifications (α, β and γ-forms) and the transformation of the different structures [2, 5, 6, 7].

* Author for correspondence: E-mail: robert.shanks@rmit.edu.au

1388–6150/2004/ $ 20.00

Akadémiai Kiadó, Budapest
Kluwer Academic Publishers, Dordrecht

Other reasons for multiple melting in polymers include the reorganization of metastable crystals [7], different crystal sizes, lamella thickening and the formation of new (secondary) crystals through annealing of specimens [2, 5, 9]. Different fractions of iPP have also been known to exhibit multiple melting peaks arising from changes in molecular mass and defects in the crystal structure due to changes in stereoregularity along the chain backbone [10].

The most common reasons for the appearance of multiple melting endotherms has been attributed to recrystallization and reorganization processes of the chain-folded lamellae during slow heating of a sample [2]. Recrystallization includes partial or complete melting of lamellae whereby chain segments are able to detach from the lateral surface of a lamella and reattach to the same or an adjacent lamella. The partially melted chain segment acquires mobility to rearrange and to attach in a more ordered configuration thereby improving the crystal structure. In comparison, reorganization is the structural changes of non-equilibrium crystals occurring in the sample in the solid-state (solid–solid transition). The lamellae may proceed to thicken in the solid phase on heating such as through sliding diffusion.

Temperature modulated differential scanning calorimetry (TMDSC) uses a periodic oscillation that is superimposed on a linear heating or cooling temperature program [10]. Additional information from the sample response to the temperature changes during transitions can be revealed. From the measured heat flow response, the total heat flow or heat capacity (C_p), such as that obtained from conventional DSC, is acquired by dividing the average heat flow or capacity by the average heating rate. Furthermore, an in-phase component, which is also referred to as reversing or storage heat capacity ($C_p^{'}$) is derived from the amplitude of the first harmonic of the Fourier transformation. It entails the heat effects associated with molecular changes that are reversible over the time and temperature of the modulation [12–14]. As such, it encompass' all the events that occur completely reversibly and some irreversible contributions. The non-reversing heat capacity (C_{pNR}) is determined from the difference between the total and reversing heat capacity.

Given that macromolecules can exhibit complex crystal structures, TMDSC can be applied in order to investigate the melting, recrystallization and reorganization behaviour that occurs on heating. TMDSC has added advantages compared with conventional DSC and these include the capability of separating thermodynamically reversible processes and kinetic contributions associated with a transition at the temperature and time of the event. For example, the glass transition can clearly be identified as it appears only in the reversing signal, separated from exothermic events such as cold-crystallization or enthalpy relaxations. Exothermic events occur only in the non-reversing signal. However, endothermic melting appears in both reversing and non-reversing signals, the extent depending on the relative state of stability of the crystals. TMDSC has been used to study the melting of many polymers including polyamide [15, 16], polycaprolactone [17, 18], polyethylene [19–22], poly[carbonyl(ethylene-co-propylene)] [23], poly(ethylene terephthalate) [24–27] and poly(oxyethylene) [19, 28].

In this study, the melting behaviour of iPP subjected to a series of thermal treatments was investigated. The temperature modulation was used as a method for crys-

tallization of the iPP, whereas melting analysis scans were performed by conventional DSC as well as TMDSC. The results provide insight into the interpretation of crystallization and melting processes studied by TMDSC and show the capability provided by combining TMDSC with conventional DSC. Treatments involved the oscillation of temperature in a saw-tooth manner, which was superimposed on a linear cooling ramp. The change in temperature amplitude, underlying cooling rate and period of modulation is expected to modify the crystallization and melting dynamics at the crystal growth front. As such, the melting response should reflect the changes that occurred during the crystallization.

Experimental

Preparation

The iPP (density=0.905 g cm^{-3}, MFI=8.5°C min^{-1}) used in this study was obtained from Qenos Pty. Ltd., (Engineering Plastics, Melbourne, Australia). The polymer was dissolved in hot xylene (138°C) and slowly precipitated in chilled acetone with continuous stirring. The fibrous mass was filtered and allowed to dry in air. The removal of lower molecular mass species and less isotactic molecules was performed by Soxhlet extraction with *n*-octane (Aldrich Chemical Co. Milwaukee, WI) for 56 h. The remaining insoluble fraction was washed with acetone and dried under vacuum. The polymer was stored in a dessicator until required.

Differential scanning calorimetry

Measurements were performed on a Perkin Elmer Pyris 1 DSC (Pyris™ software version 3.81) operating at ambient mode, with ice–water slurry (2–5°C) as a coolant source. The enclosed chamber was purged with dry nitrogen at a flow rate of 20 mL min^{-1}. The instrument was calibrated for temperature and enthalpy with high purity indium (156.60°C, 28.45 J g^{-1}) and zinc (419.47°C, 108.37 J g^{-1}) standards. The calibration was periodically checked *vs.* the onset of melting for indium. Specimens of the extracted iPP were weighed (2–3 mg) using a Perkin Elmer microbalance (AD-2Z Autobalance) calibrated using standard milligram masses. The specimens were encapsulated in standard hermetically sealed aluminium pans (30 μL).

The samples were heated to 210°C and held for 5 min to eliminate incipient nuclei prior to crystallization and destroy the ordered regions (helical structure) in the melt that could exist above the melting temperature of iPP [28]. A series of temperature profiles were used to thermally treat the iPP and these are listed in Table 1. The first 5 profiles utilized a saw-tooth modulation, which consisted of linear segments of cooling and heating (30 s each segment) in the Pyris 1 DSC capable of TMDSC function. The treatment will also be referred to as modulated cooling (MC). The rate of cooling (β_1) and heating (β_2) are also indicated in the table. The period of modulation (per) was 60 s except for profile 4 where per=120 s. The underlying cooling rate (β_0) was maintained at 2°C min^{-1} with a decreasing modulation temperature amplitude

(T_a) for profiles 1–3. Profiles 4 and 5 have β_0 reduced to 1°C min^{-1}. Each treatment concluded at 20°C. Standard melting curves were obtained from 20 to 200°C at the heating rates of 10 and 2°C min^{-1}. Fresh samples taken from the Soxhlet extracted *n*-octane iPP were used in each cooling treatment profile to avoid any thermal history effects that could result from previous thermal treatments. A baseline scan was performed using a matched empty pan under the same conditions. The degree of crystallinity (χ) of iPP was calculated on the basis that iPP with crystallinity of 100% has enthalpy of melting (ΔH_0) of 209 kJ kg^{-1} as indicated by the following relationship where ΔH_m is the measured melting enthalpy [30]:

$$\chi = \frac{\Delta H_m}{\Delta H_0} \quad (1)$$

Table 1 Crystallization treatment of PP, modulated cooling (cool–heat) and linear cooling

Profile	T_1/°C	T_2/°C	T_3/°C	β_1/ °C min^{-1}	β_2/ °C min^{-1}	β_0/ °C min^{-1}	per/s	T_a/°C
1	210	205	208	10	6	2	60	2.0
2	210	206	208	8	4	2	60	1.5
3	210	207	208	6	2	2	60	1.0
4	210	207	208	3	1	1	120	1.0
5	210	208	209	4	2	1	60	0.75
6						2		

The TMDSC melting scan of iPP with selected treatments (profiles 1, 3, 4 and 6 of Table 1) was performed by heating the samples using modulated heating from 20 to 200°C. The underlying heating rate was 2°C min^{-1}, per=60 s (frequency of 16.7 mHz) and T_a=1.5°C. A baseline scan was obtained with an empty pan under the same conditions. The measured heat flow data was then used to calculate the total C_p, reversing and non-reversing C_p.

Quasi-isothermal (QI) measurements were performed at selected temperatures in the range of 50 to 180°C, as determined from a melting endotherm of the extracted iPP, cooled at a rate of 10°C min^{-1} followed by the same heating rate. The temperature amplitude was 1.5°C, per=60 s (frequency of 16.7 mHz) and zero underlying heating rate [30]. The last 10 min of the 20 modulation cycles was used to determine C_p'. Lissajous figures were constructed to monitor the approach to steady state.

Results and discussion

DSC – conventional heating

Temperature modulated cooling (MC) was used to thermally treat iPP in order to allow the lamellae to approach closer to equilibrium. Figure 1 shows the melting

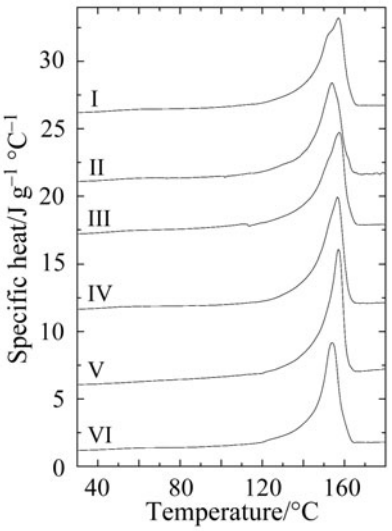

Fig. 1 Specific heat melting curves obtained at 10°C min^{-1} for iPP crystallized under modulated and linear cooling. The crystallization conditions are: curves I–III; per=60 s, T_a=2.0, 1.5 and 1.0 and β_0=2.0°C min^{-1}, curves IV and V; per=120, 60 s, T_a=1.0, 0.75, respectively and β_0=1.0°C min^{-1}. Reference curve VI has linear cooling at a rate of 2°C min^{-1}. The curves have been displaced 5 units consecutively

endotherms obtained at 10°C min^{-1} for iPP that was subjected to various cooling treatments. Curves I–V correspond to the modulated cooling treatment as detailed in Table 1 and curve VI serves as a reference with only a slow linear cooling treatment at 2°C min^{-1}. The reference curve (VI) shows a relatively sharp, narrow single peak with a melting peak temperature (T_m) at 153.9°C (Table 2) while the final melting temperature ($T_{m\,f}$) of the crystals on return to the baseline (±0.01 J g^{-1}) was 164.9°C. The crystallinity for linearly cooled iPP was determined to be 0.45. For modulated cooling where the underlying rate was 2°C min^{-1} and T_a was modified from 2.0 to 1.0°C (curves I–III), the melting endotherm was notably altered by the additional oscillation in temperature. The larger T_a (2.0°C) resulted in a broadening of the endotherm with main melting peak appearing at 157.0°C and a shoulder centering at 153.0°C. The melting peak shape indicates that a broader range of lamella thickness formed in the sample during temperature modulated cooling. Even so, the last trace of melting was shifted almost 2°C to higher temperature, evidence that the formation of thicker lamellae and more organized crystals occurred by this cooling treatment as compared with linear cooling. However, some recrystallization can occur giving rise to melting at higher temperature, the extent changing with heating rate as will be discussed later. Curves II and III, both show broadening and it appeared that with a T_a of 1.5°C, the melting dominated at lower temperature, but a slight shoulder is still seen on the higher temperature side of the endotherm. In contrast, the lowest T_a of 1.0°C shows a similar melting endotherm as seen in curve I with melting dominating toward higher temperature. Both these treatments have thermodynamically stable

crystals under these conditions that conclude their melting at even higher temperature, in this case the shift is by 2.0 to 3.3°C. The subtle differences in T_a have markedly influenced the crystals formed and hence the melting endotherm of iPP observed. The lowest T_a as indicated from these results, produces crystals of relatively higher stability since most of the melting occurs at higher temperature.

An increase in the enthalpy of melting and therefore the degree of crystallinity, also signified an improvement of crystal structure. The greatest increase was observed for profile 3 (curve III), where the change in temperature amplitude was the smallest. The crystallinity was increased from 0.45 for conventional linear cooling to 0.53 for modulated cooling. This implied that the smaller amplitude induced by the modulation would enable thickening of lamellae at the surfaces to be enhanced, resulting from a less extreme temperature difference experienced by the sample during the overall cooling.

The fluctuation in temperature affects the nucleation and growth rate of crystallization in each modulation cycle. From the melt state, the nucleation induction time for nuclei formation may be increased. If a nucleus formed during a cooling segment is lower than the critical size, then it will be thermodynamically unstable and melt during the heating segment. This would add to the thermodynamic and kinetic energy barriers imposed on the nucleation of the polymer. In addition, nuclei that are greater than the critical size will remain stable while they are incrementally heated in the cycle. On cooling, crystal growth will be encouraged [31, 32]. It is known that crystal growth is sensitive to these changes in temperature. The smaller change in temperature will not perturb the growth as much and therefore molecules in the melt that approach lateral surfaces of growing crystal lamellae, may attach in a more favourable molecular configuration. This is aided by the slower cooling rate (β_1) in the cooling portion of the cycle in conjunction with the already relatively slow average cooling rate (β_0). Faster cooling rates and therefore shorter time spent at each temperature may lead to the formation of less ordered lamellae because of the time limitation and alterations to the kinetics of crystallization and melting dynamics. Although a general increase in the crystallinity is seen relative to the linear cooling, the larger T_a would lessen the efficiency of the chain segments to become attached and pack in the crystalline structure.

Table 2 Melting characteristics of modulated and linearly cooled iPP obtained at 10°C min^{-1}

Profile[a]	$T_{m\ onset}$/ °C	T_m/ °C	T_{mf}/ °C	ΔH_m/ J g^{-1}	χ	Peak height/ J g^{-1} °C^{-1}
1	142.7	157.0	166.8	109.3	0.52	6.5
2	142.5	153.8	168.2	108.9	0.52	6.8
3	144.8	157.4	167.1	110.4	0.53	6.9
4	143.3	156.6	167.7	114.3	0.55	7.9
5	149.3	157.1	165.2	108.4	0.52	9.1
6	145.7	153.9	164.9	97.9	0.45	7.4

[a] Corresponds the experimental parameters as detailed in Table 1

Curves IV and V in Fig. 1 represent the melting for profiles 4 and 5, respectively from Table 1. In this case, the average cooling rate has been reduced to 1°C min^{-1}, which effectively increase the time available for the iPP to crystallize and to perfect the lamellae structure. Both these endotherm curves show single peaks. However, curve V exhibits a sharper, narrower peak complimented by a marked increase in peak height of 9.1 J g^{-1} $°C^{-1}$. This was considerably greater than the previous modulated cooling treatments, may indicate a larger crystal population with more uniform lamella thickness. Although the average cooling rate and temperature amplitude were the lowest of the series, the crystallinity and the last trace of crystal melting detected, was similar to that obtained for profiles 1–3. In addition, profile 4 exhibited the highest crystallinity of 0.55, however the melting endotherm was broader on the lower temperature side. The differences may be attributed to the change in frequency, that is, the sample treatment using profile 5 undergoes two modulation cycles in the time one cycle is completed for profile 4.

The curves displayed in Fig. 2 were obtained by heating at 2°C min^{-1}, similar to the average rate of cooling. The reference curve (VI) exhibited a double melting endotherm with T_m appearing at 155.5 and 161.5°C as recorded in Table 3. The lower melting peak can be attributed to the melting of the originally crystallized material formed on cooling, while the second peak at higher temperature is due to the melting of recrystallized/reorganized lamellae on slow linear heating. This melting phenomena is seen in many polymers including syndiotactic PP [34], polystyrene [35, 36], polyamide [37], poly(ethylene terephthalate) [38] and polyethylene [39]. The effect

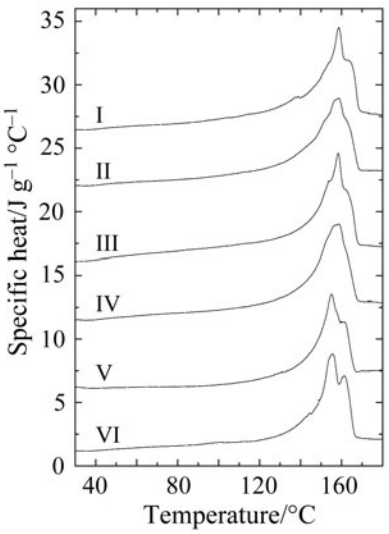

Fig. 2 Specific heat melting curves obtained at 2°C min^{-1} for iPP crystallized under modulated and linear cooling. The crystallization conditions are: curves I–III; per=60 s, T_a=2.0, 1.5 and 1.0 and β_0=2.0°C min^{-1}, curves IV and V; per=120, 60 s, T_a=1.0, 0.75, respectively and β_0=1.0°C min^{-1}. Reference curve VI has linear cooling at a rate of 2°C min^{-1}. The curves have been displaced 5 units consecutively

of heating rate on the melting of iPP has been shown to modify the observed melting. Yadav *et al.* [2] report that with decreasing heating rates, the magnitude of the second peak increases at the expense of the first. Comparing the reference curves (VI) of both Figs 1 and 2, these results follow what is generally agreed upon.

Table 3 Melting characteristics of modulated and linearly cooled iPP obtained at 2°C min^{-1}

Profile[a]	$T_{m\ onset}$/ °C	T_m/ °C	T_{mf}/ °C	ΔH_m/ J g^{-1}	χ	Peak height/ J g^{-1} °C^{-1}
1	152.5	158.7	171.4	122.9	0.59	6.8
2	146.3	157.5	169.9	124.2	0.59	5.8
3	151.6	158.4	169.3	128.6	0.61	7.3
4	140.2	158.7	168.9	116.2	0.56	6.2
5	147.5	155.1	167.3	97.5	0.46	6.3
6	145.5	155.5, 161.5	169.1	111.9	0.54	6.9

* Corresponds the experimental parameters as detailed in Table 1

The corresponding melting curves for cooling profiles 1–3 display complex endotherms (curves I–III). Common to all three curves is the appearance of the main melting peak at about 158°C, almost midway between the two peaks observed for the linearly cooled iPP (curve VI). In addition, a slight broad shoulder on the lower temperature side and a pronounced shoulder on the higher temperature side are noted. The peak temperatures are slightly higher than those of the previous series (compare with Table 1), however the melting is much broader. Given that the average cooling rate is identical for these profiles, a larger and more pronounced shoulder was observed for larger T_a (curve I) implying more recrystallization/reorganization took place on heating. $T_{m\,f}$ was found to shift about 2°C to higher temperature for all profiles compared with curve VI, with larger T_a shifting most (refer Table 3). A notable increase in the enthalpy of melting was observed, not only from the use of a slower heating rate, but also compared with the reference curve of this series. The endotherm of the reference curve resulted in ΔH_m=111.9 J g^{-1} and it was found to increase in ΔH_m for curves I–III to at least 122.9 J g^{-1}. With decreasing T_a, there was a further increase as listed in Table 3, with curve III exhibiting the largest degree of crystallinity. The slower underlying heating rate has enabled further changes to take place in the sample during heating.

Curves IV and V in Fig. 2 also show broad melting endotherms, particularly for the former. There appears to be little distinction in the formation of a shoulder on the higher temperature side, which is obscured by the broad main melting at 158.7°C. $T_{m\,f}$ also was similar to the previous three curves. The enthalpy was only marginally increased compared with the reference, but somewhat lower than that obtained for profiles 1–3 (refer Table 3). Similarly for curve V (profile 5), the iPP exhibited a peak at 155.1°C and a broad shoulder at higher temperature. The enthalpy measured appeared to be much lower than expected. This may be attributed to the relatively large T_a for the underlying cooling rate used in conjunction with the slow heating rate. The crys-

tals that have formed during crystallization have limited ability to recrystallize/reorganize on heating because the relative thermodynamic stability should be much greater than those of profiles 1–3.

Increased perfection of crystallites has also been observed for samples of poly(*p*-phenylene sulfide) by Menczel, who subjected samples to conventional and temperature modulated cooling by cool–heat methods [40]. The author found that the crystallinity remained constant and although the melting peak temperature was decreased as a result of the modulation, the temperature of the final remaining crystals shifted significantly to higher temperature. Here, we have observed modification to the melting peak shape, position and changes in enthalpy, which show that the degree of crystallinity can be increased by using temperature modulated cooling as a method of sample treatment for iPP.

TMDSC – modulated heating

To extend on the investigation of modulated cooling on the resulting melting endotherms, TMDSC was employed to further elucidate multiple melting behaviour observed for iPP. As described in the method, MC using profiles 1, 3 and 4 were adopted as well as linear cooling thermal history (profile 6). The MC modified the structure and crystallinity of the crystals that form during crystallization. On heating, the amount of recrystallization/reorganization is affected by both the temperature and time. Less well organized lamellae from the melt are expected to exhibit a larger contribution to reversible melting during heating [20, 22, 41].

The first series of melting curves presented in Fig. 3a are the total specific heat curves obtained by TMDSC. All the curves show multiple melting endotherms, with a similar profile to that obtained with linear heating at 2°C min^{-1} (compare with curve VI in Fig. 2). The reference in this figure is curve IV and it appears that much of the sample has undergone recrystallization/reorganization on heating, as indicated by the larger peak that occurred at higher temperature. The double melting endotherm observed for MC profile 1 appears most resolved, particularly for the higher melting peak. From Table 4, it can be seen that the melting peak temperature for the first peak was 154.2°C and the second at 161.3°C. Curves II and III show similar peak shapes, however, the relative magnitude of the peak height has been altered. The melting of the original crystals formed using MC profile 3 (curve II), has shifted the melting peak to 156.3°C, while the higher melting peak appeared at 160.4°C, somewhat lower than that in curve I. This is attributed to the change in temperature amplitude affecting the stability of crystals formed. It was also noted that for curve II, a gradual exotherm before the main melting appears, indicating some further reorganization on heating. The resulting melting endotherm for profile 4 (curve III) appears as the broadest of all the modulated cooled profiles. From the crystallinity of the samples, MC profile 1 gave the same result as that of the linearly cooled sample. The other two MC profiles show a much reduced crystallinity, even when compared with those listed in Table 3. This may be due to the added complexity involved with the modulated heating of the samples and its affect on melting and crystallization processes.

Table 4 Temperature modulated melting properties of iPP with modulated and slow cooling

Profile[a]	$T_{m\ onset}$/ °C	T_m/ °C	T_{mf}/ °C	ΔH_m/ J g^{-1}	χ	$T_m(C_p')$/ °C	$\Delta H_m(C_p')$/ J g^{-1}	χ	$\Delta H_m(C_p')/\Delta H_m$	$T_m(C_{pNR})$/ °C	$\Delta H_m(C_{pNR})$/ J g^{-1}
1	147.4	154.2, 161.4	171.1	109.3	0.52	153.9	64.2	0.21	0.59	154.1, 161.7	65.5
3	148.8	156.3, 160.4	168.5	96.0	0.46	154.1	39.6	0.13	0.41	156.4, 162.3	76.9
4	145.9	156.3, 161.9	170.2	97.5	0.47	155.3	42.5	0.14	0.44	156.4, 162.0	43.9
6	144.7	~155, 160.3	169.6	108.4	0.52	152.2	43.8	0.14	0.40	154.3, 160.5	57.4

[a] Corresponds the experimental parameters as detailed in Table 1

The reversing specific heat curves shown in Fig. 3b reveal that iPP exhibits a reversible contribution during heating over the time and temperature of the measurement. Melting of the primary and secondary crystals within each modulation as well as reversible melting (melting, recrystallization and remelting) at the lamellae sur-

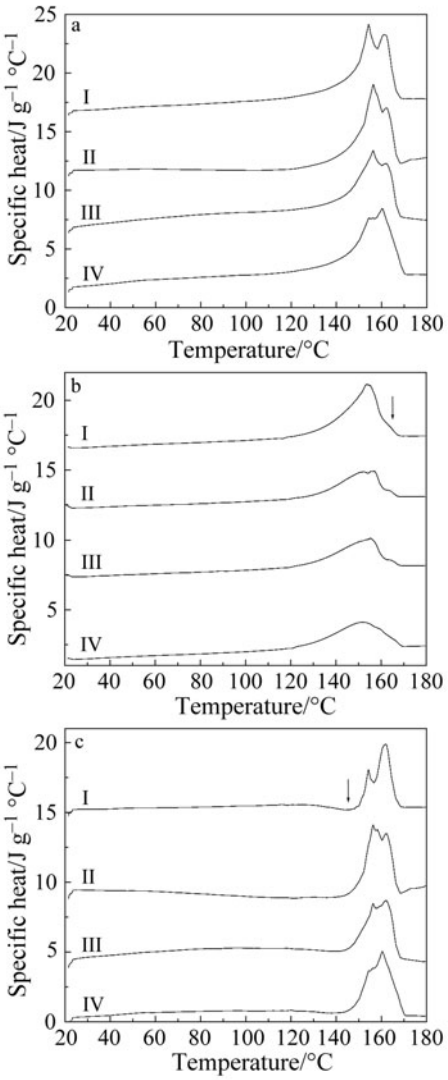

Fig. 3 TMDSC specific heat melting curves of iPP after modulated cooling. a – Total, b – reversing and c – non-reversing specific heat. Heating parameters: per=60 s, T_a=1.5 and β_0=1.0°C min^{-1}. Crystallization conditions curve I, II; per=60 s, T_a=2.0 and 1.0°C and β_0=2.0°C min^{-1}. Curve III; per=120 s, T_a=1.0°C and β_0=1.0°C min^{-1}. Reference curve IV has linear cooling at a rate of 2°C min^{-1}. The curves have been displaced 5 units consecutively

faces [25, 26] can occur. The contribution begins to take place when increasing temperature induces adequate molecular motions in the sample. The chain segments that are attached to a lateral crystal surface of lamellae may become detached and enable rearrangement to a more stable conformation [43]. A chain segment then can reattach to the same or an adjoining crystal surface with the exothermic energy released contributing to the non-reversing signal. Under the conditions of continual increasing temperature, truly thermodynamic reversible melting cannot be obtained because of the superimposing effects of irreversible processes (recrystallization, annealing and melting). This is discussed later for quasi-isothermal measurements on iPP.

For the iPP in all cases, the magnitude of the reversible contribution increased with increasing temperature, with most occurring in the main melting peak region of the total specific heat. All of the curves exhibited a broad endotherm, with the peak temperature remaining at about 154°C (refer Table 4). On the higher temperature side of the endotherm, a small shoulder is evident (indicated by an arrow in Fig. 3b) and represents the final stages of reversible melting contribution of the more ordered crystals taking place. It appears most pronounced in curve I (profile 1). These observations indicate that reversible melting primarily occurs in the main melting region, in particular that corresponding to first peak of the total specific heat curve. As more of the existing lamellae in the crystals thicken, the relative amount of the reversible contribution decreases. This is shown by the lower reversible contribution at higher temperature whereby most of the lamellae melt. This is not only due to the higher melting crystals produced, but also as a result of increasing temperature that eventuates in the complete melting of crystals entities. The enthalpy of the reversing specific heat contribution is indicated in Table 4. As expected, it is lower than that obtained for the total specific heat. The fraction is given as $\Delta H_m\,(C_p^{'})/\Delta H_m$ in each case. The relative proportion for the reference with 2°C min^{-1} linear cooling was 0.40. The modulation in temperature resulted in an increased proportion of reversible melting. Profile 1 with largest T_a of 2°C had the largest fraction (0.59) of lamellae that underwent reversible melting during heating indicating more unstable crystals in the sample. Whereas, profiles 3 and 4 only showed a small relative increase resulting from further changes, but not to the same extent as profile 1. The lowering of the relative fraction of reversible melting has been attributed to the lower T_a (profile 3) and further decrease in the average underlying cooling (profile 4). This indicates that the crystals formed with profile 1 are relatively less thermodynamically stable than those formed with lower temperature amplitude. This supports the view that larger T_a produces crystals that are not as well formed as previously mentioned.

The non-reversing specific heat curves displayed in Fig. 3c show that endothermic melting dominates any other changes that occur in the sample. This indicates that much of the melting is irreversible and suggests that most of the energy goes into the disruption of the crystal structure, typically due to the complete melting of lamellae. Before the main melting region of the curves, a slight exothermic contribution due to reorganization appears [42]. This is indicated by an arrow for curve I, but similarly occurs for the other treated samples. Since melting, recrystallization and reorganization occur in the sample all while heating, the processes may not be easily separated

and therefore are partly obscured by competing events. The recrystallization rapidly proceeds due to the already present crystal surfaces acting as a template, even with no localized cooling [42]. Contrary to crystallization nucleation (homogeneous) is necessary, whereas recrystallization does not require molecular nucleation and therefore the process is not kinetically hindered by diffusion hence the activation energy is lower [22]. Therefore, it can be noted that, the behaviour of iPP crystal entities undergoes melting, recrystallization/reorganization and remelting processes during heating. For the reference (Fig. 3c, curve IV), the relative magnitude of the second melting peak is larger than the first indicating that the melting of the more ordered lamellae in the crystals is mostly irreversible at the temperature and time scale of the experiment. This was similar for iPP that underwent MC profile 1. However, curve I shows more clearly defined peaks, with the first melting peak smaller in magnitude than the higher melting peak. This may indicate that further changes in the sample occurred during the heating as T_a was larger during MC. Profiles 3 and 4 show complex endotherms with the peaks appearing less defined and similar in magnitude. Common to both are the melting peaks at about 156 and 162°C.

As described previously, the reversing component encompasses various contributions under the modulation conditions applied. Quasi-isothermal experiments can be used to measure the contribution arising from the changes occurring with the modulation after irreversible effects have completed under the particular conditions. Such irreversible effects include the partial melting of thinner crystals, which may recrystallize/reorganize to form crystals of increased thickness. This may proceed given that molecular nucleation can occur from crystal species still present at the temperature and time. It has been suggested that this is possible for iPP [44]. In addition, some polymers are capable of undergoing a chain sliding mechanism (longitudinal chain diffusion) to thicken crystals, which is more likely to occur for linear molecules such as PE and POE. This mechanism would be less prevalent in iPP given that the methyl group presents a physical limitation.

From the quasi-isothermal measurements, the heat flow was greater when more changes were occurring in the sample and a larger C_p' contribution was observed, particularly in the main melting region of the endotherm. Progressing with time there was a decrease at each temperature because irreversible events in the sample no longer followed the modulation. Lissajous figures (normalized heat flow *vs.* normalized temperature) indicated the establishment of a new steady state with each increase in base temperature. The reversing contribution of iPP crystallized at 10°C min^{-1} is shown in Fig. 4. It is seen that a minor contribution of the total melting is reversible melting that follows the modulation (29%). It would be expected that the proportion would be less for iPP crystallized at a much slower rate.

Wunderlich *et al*. have suggested six contributions to the heat capacity [20–23]. The vibrational and conformational motions including the true reversible melting are truly thermodynamically reversible. Primary and secondary crystallization along with crystal perfection all have different degrees of irreversibility. For polymers, the first contribution is always vibrational and forms the largest component of the heat capacity. The second contribution arises from the dynamically changing conformational isomers. This includes cooperative rotational motion that may proceed along the backbone carbon atoms, even

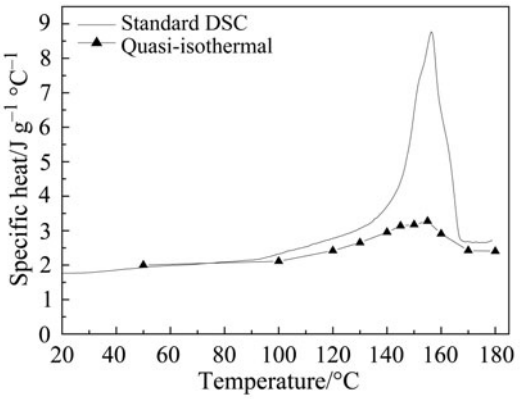

Fig. 4 Specific heat curves for standard DSC (solid line) and quasi-isothermal measurements (symbol) over the melting range. Parameters; T_a=1.5°C and per=60 s for the duration of 20 min. The last 10 modulation cycle data was used for the calculation

within a crystal. PE has a greater capability to undergo changes in conformation compared with iPP. The methyl side group along the backbone restricts rotation within a crystal and the associated potential energy would be much higher. The third contribution, reversible melting was observed to occur in iPP. Not all melting requires the complete removal of molecules from a crystal. Semicrystalline polymers show the ability for sections of molecules to partially melt and become detached from the surface of a crystal. With the modulation in temperature, they may recrystallize and melt reversibly. With increasing temperature however, the melting becomes more irreversible as the molecules are not able to reattach themselves to a crystal surface and therefore remain in the melt state. Crystals (lamellae surfaces) are necessary to prevent primary and secondary nucleation. In addition, molecular nuclei are required to initiate the reversible process [45]. Crystal perfection encompasses annealing and/or changes that occur on heating, which enables the lamellae to be improved with the extent having temperature and time dependence. The relative thermal stability of the lamellae increases and melting becomes shifted to higher temperature [22].

TMDSC has been useful in revealing further information on the melting processes that occur while heating. Much of the melting is irreversible, as the proportion of the non-reversing specific heat is much greater than that of the reversing contribution. Similar observations have been noted by Androsch *et al*. [44, 46]. In their investigation, iPP that was more rapidly cooled (quenched) was found to exhibit a reversing contribution, which began above the glass transition, whereas a sample crystallized at a slower rate (10°C min^{-1}) showed a lower contribution within the modulation conditions. Here, we have observed that the relative state of the crystals formed under modulated cooling conditions exhibited in general a lower reversing contribution with slower underlying cooling rate and temperature amplitude.

Conclusions

The crystallinity of an *n*-octane extracted iPP was increased significantly by using modulated temperature methods for cooling the polymer. Conventional cooling at 10°C min^{-1} yields χ ~0.45 while a slower heating rate after the same thermal history increased this slightly to 0.47 (2°C min^{-1}). The modulation experienced by the sample on cooling has been shown to increase the crystal order, leading to higher melting temperatures and much improvement in the crystallinity. In summary, for a change in the amplitude of the modulation, greater improvement was achieved for a lower magnitude change in temperature as seen for MC profiles 1–3. The change in the average cooling rate from 2 to 1°C min^{-1} did show some improvement, however it was limited (profiles 4 and 5). With the change in heating rate from 10 to 2°C min^{-1}, the increase in time available resulted in further structural ordering through recrystallization and reorganization of lamellae on heating. The iPP endotherm after modulated cooling exhibited main melting at higher temperature, in addition to a shoulder that formed from these phenomena. The shift in the melting of the last traces of crystals detected at high temperature also signifies that the formation of thicker lamellae can form and is promoted with slower heating rates. In regards to the greatest increase in crystallinity for iPP, MC profile 3 with lowest T_a of 1.0°C, in conjunction with slow heating rate of 2°C min^{-1}, had improved the structure and resulted in the χ=0.61. Multiple melting behaviour commonly observed for iPP has been probed by TMDSC. Melting of the crystals predominates (non-reversible contribution), however a smaller reversing contribution was also detected indicating more subtle changes occurred in the main melting range while heating.

* * *

One of the authors (A. G.) acknowledges the receipt of an Australian Postgraduate Award (APA) during this project. Special thanks are given by the authors to Dr. Gandara Amarasinghe for suggestions and discussion in the preparation of this manuscript.

References

1 K. D. Pae, J. Polym. Sci., 6 (1968) 657.
2 Y. S. Yadav and P. C. Jain, Polymer, 27 (1986) 721.
3 R. J. Samuels, J. Polym. Sci. Polym. Phys. Ed., 13 (1975) 1417.
4 Y. C. Kim, W. Ahn and C. Y. Kim, Polym. Eng. Sci., 37 (1997) 1003.
5 W. W. Cox and A. A. Duswalt, Polym. Eng. Sci., 7 (1967) 309.
6 J. G. Fatou, Eur. Polym. J., 7 (1971) 1057.
7 J. Varga and A. Menyhard, J. Therm. Anal. Cal., 73 (2003) 735.
8 P. B. Rim and J. P. Runt, Macromolecules, 16 (1983) 762.
9 P. D. Calvert and T. G. Ryan, Polymer, 25 (1984) 921.
10 R. Paukkeri and A. Lehtinen, Polymer, 34 (1993) 4083.
11 M. Reading, J. Therm. Anal. Cal., 64 (2001) 7.
12 R. Scherrenberg, V. Mathot and A. Van Hemelrijck, Thermochim. Acta, 330 (1999) 3.

13 S. Swier, G. Van Assche, A. Van Hemelrijck, H. Rahier, E. Verdonck and B. Van Mele, J. Therm. Anal. Cal., 54 (1998) 585.
14 P. S. Gill, S. R. Sauerbrunn and M. Reading, J. Thermal Anal., 40 (1993) 931.
15 A. Toda, C. Tomita and M. Hikosaka, J. Therm. Anal. Cal., 54 (1998) 623.
16 L. Judovits, J. D. Menczel and A. G. Leray, J. Therm. Anal. Cal., 54 (1998) 605.
17 J. E. K. Schawe, E. Bergmann and W. Winter, J. Therm. Anal. Cal., 54 (1998) 565.
18 A. Toda and Y. Saruyama, Polymer, 42 (2001) 4727.
19 W. Hu, T. Albrecht and G**.** Strobl, Macromolecules, 32 (1999) 7548.
20 R. Androsch, Polymer, 40 (1999) 2805.
21 R. Androsch and B. Wunderlich, Macromolecules, 32 (1999) 7238.
22 R. Androsch and B. Wunderlich, Macromolecules, 33 (2000) 9076.
23 M. Pyda, M. L. Di Lorenzo, J. Pak, P. Kamasa, A. Buzin, J. Grebowicz and B. Wunderlich, J. Polym. Sci: Part B: Polym. Phys., 39 (2001) 1565.
24 S. Montserrat, F. Roman and P. Colomer, J. Therm. Anal. Cal., 72 (2003) 657.
25 I. Okazaki and B. Wunderlich, Macromol. Rapid Commun., 18 (1997) 313.
26 I. Okazaki and B. Wunderlich, Macromolecules, 30 (1997) 1758.
27 M. Song, J. Appl. Polym. Sci., 81 (2001) 2779.
28 K. Ishikiriyama and B. Wunderlich, Macromolecules, 30 (1997) 4126.
29 X. Zhu and D. Yan, Macromol. Chem. Phys., 202 (2001) 1109.
30 R. P. Quirk and A. A. Alsamarraie, Physical Constants of Poly(propylene), in Polymer Handbook, J. Brandrup and E. H. Immergut, (Eds), Wiley, New York 1989, p. V/27.
31 K. Ishikiriyama and B. Wunderlich, J. Polym. Sci: Part B: Polym. Phys., 35 (1997) 1877.
32 Y. Long, R. A. Shanks and Z. H. Stachuski, Prog. Polym. Sci., 20 (1995) 651.
33 E.-Q. Chen, X. Weng, A. Zhang, I. Mann, F. W. Harris, S. Z. D. Cheng, R. Stein, B. S. Hsiao and F. Yeh, Macromol. Rapid Commun., 22 (2001) 611.
34 J. Xu, L. Feng, Z. Liu, Y. Deng, C. Cui and W. Chen, Polym. Int., 48 (1999) 53.
35 T. Liu, S. Yan, M. Bonnet, I. Lieberwirth, K.-D. Rogausch and J. Petermann, J. Mater. Sci., 35 (2000) 5047.
36 Z. Yuan, R. Song and D. Shen, Polym. Int., 49 (2000) 1377.
37 Y. Li, X. Zhu, G. Tian, D. Yan and E. Zhou, Polym. Int., 50 (2001) 677.
38 S. Tan, A. Su, W. Li and E. Zhou, J. Polym. Sci. Part B: Polym. Phys., 38 (2000) 53.
39 R. G. Alamo, R. H. Glaser and L. Mandelkern, J. Polym. Sci. Polym. Phys. Ed., 26 (1988) 2169.
40 J. D. Menczel, J. Therm. Anal. Cal., 58 (1999) 517.
41 R. Androsch, J. Polym. Sci: Part B: Polym. Phys., 39 (2001) 750.
42 B. B. Sauer, W. G. Kampert, E. N. Blanchard, S. A. Threefoot and B. S. Hsiao, Polymer, 41 (1999) 1099.
43 J. Schmidtke, G. Strobl and T. Albrecht, Macromolecules, 30 (1997) 5804.
44 R. Androsch and B. Wunderlich, Macromolecules, 34 (2001) 8384.
45 B. Wunderlich, Macromolecular Physics, Vol. 2, Academic Press, New York 1976.
46 R. Androsch and B. Wunderlich, Macromolecules, 34 (2001) 5950.